

Ultrasound Allied Laser Sono-photobiomodulation Activated Nano-curcumin: Up-and-Coming Selective Cancer Cell Killing Modality

Samir Ali Abd El-Kaream (✉ Samir_ali852006@yahoo.com)

Medical Research Institute, Alexandria University, Egypt

Hoda Abdelrahman Mohamed

Medical Research Institute, Alexandria University, Egypt

Sohier Mahmoud El-Kholey

Medical Research Institute, Alexandria University, Egypt

Mahmoud Matar Mohammad Abu Rakhey

Qilu Hospital of Shandong University

Amin M Said ELkallaf

Medical Research Institute, Alexandria University, Egypt

Amal Saleh Mohamed Soliman

Alexandria Higher Institute of Engineering and Technology

Marwa Ahmed Khodary

Alexandria Higher Institute of Engineering and Technology

Research Article

Keywords: nano-curcumin, implanted tumor, sonodynamic therapy, photobiomodulation therapy

Posted Date: September 14th, 2022

DOI: <https://doi.org/10.21203/rs.3.rs-2054679/v1>

License: © ⓘ This work is licensed under a Creative Commons Attribution 4.0 International License.

[Read Full License](#)

Abstract

The purpose of this study was to assess the effectiveness of activated nano-curcumin as a cancer-targeted therapy. Six groups of albino mice with cancer implants were used for this study. Sono- (ultrasound) and photo- (blue laser) were used as energy sources. The outcomes showed that nano-curcumin is an effective photo-sono sensitizer for the treatment of cancer. Upon activation with blue laser and/or ultrasound, nano-curcumin plays a crucial part in inhibiting tumor development and promoting cancer cell death. Our findings showed that activated nano-curcumin might be used as a natural nanosensitizer for cancer targeted sono-photobiomodulation therapy (SPBMT).

Highlights

1. New trend of cancer treatment: sono-photo-biomodulation therapy (SPBMT) in combination with nano-curcumin as a sono-photo-sensitizer.
2. A phytochemical nanomaterial with great potential as effective drug delivery targeting system for SPBMT.
3. Nontoxic, safe and locally activated cancer treatment modality.
4. Selective cancer killing.

Introduction

Without a question, one of the most challenging research topics is cancer. It is widely accepted that tumors can be treated using traditional treatment options such chemotherapy, radiation, surgery, and combination therapy in order to cure or eradicate them. Chemotherapy is still a very effective cancer treatment option however it comes with an excessive amount of dangers and unfavorable side effects. There is always a chance of recurrence, and some cancers could acquire resistance to chemotherapy and radiation treatment. One must look for fresh therapeutic solutions in order to treat tumors successfully and prevent the spread of cancer. So to overcome the main obstacles involved in traditional cancer treatment, researchers are looking for effective treatments in alternative, complementary medicine and supplements [1,2].

Photodynamic therapy (PDT) treatment method has been established to treat different kinds of cancers. PDT involves a photo-sensitive drug intake and the affected area subsequently illuminated with light corresponding to the sensitizer absorbance wavelength. Factors that govern PDT cancer therapy; include the photosensitizing agent localization in cancerous tissue and the appropriate light dose delivered to that tissue [3,4].

Sonodynamic therapy (SDT) treatment method evolved from PDT to overcome the light drawbacks penetration depth. SDT involves a sono-sensitive drug intake and the target area subsequently exposed to ultrasound. Using SDT enabled penetration of up to several tens of centimeters of tissue. Consequently, SDT put an end to PDT obstacles and major limitations. [5–7].

Sono-photobiomodulation therapy (SPBMT) is a treatment method that includes photo- and sono-sensitive agents. PDT has been conducted separately away of SDT for years with variable success for cancer treatment. PDT has been directed for superficial cancer, while upon the combination with SDT, it showed to be functional for deep tumors and metastatic cancer when spread to the lung, liver, and bone in particular [6,7].

Curcumin (CUR) sparingly soluble polyphenolic compound with poor solubility and absorption derived from the root of *Curcuma longa*. Commercially available curcumin is diferuloylmethane, bisdemethoxycurcumin, and demethoxycurcumin combinations owing to that nanoparticle enable greater solubility and absorption rate. Researchers provided evidence that curcumin has antibacterial, antifungal, antiviral, antioxidative, anti-inflammatory, and antiproliferative moieties [8–11].

Our work aimed at study the antitumor potential of photobiomodulation and sonodynamic therapy combined with nano-curcumin sensitizer on the Ehrlich tumor implanted in mice. To attain our goal, the following steps have been done:

Materials And Methods

Preparation of nano-curcumin

In the current work, nano-curcumin was employed as SPS. Nano-curcumin was prepared by the solvent-antisolvent precipitation ultrasonication method [12]. To all tumor-bearing mice, treated groups, nano-curcumin was administered by intraperitoneal (ip) injection 9–12 hrs before exposure to PDT and/or SDT for two weeks.

Experimental protocol

130 male albino mice bearing EAC carcinoma. Upon 10 days of tumor inoculation, the tumor reached about 1mm, the study treatment started. The present study protocol was conducted following the ethical guidelines. Experimental animals were subdivided into

G I: 10 mice: normal with no tumor (negative control), 10 mice: mice inoculated with EAC without treatment (positive control) and 10 mice: mice inoculated with EAC treated with nano-curcumin without activation.

G II: 10 mice: EAC-bearing mice irradiated with blue Laser, low frequency, for 3 minutes and 10 mice: EAC-bearing mice irradiated with blue Laser, high frequency, for 3 minutes.

G III: 10 mice: EAC-bearing mice irradiated with puls US for 3 minutes and 10 mice: EAC-bearing mice irradiated with cont US for 3 minutes.

G IV: 20 mice: EAC-bearing mice treated with (nano-curcumin) were irradiated with laser light as same G II conditions.

G V: 20 mice: EAC-bearing mice treated with (nano-curcumin) were irradiated with ultrasound as same G III conditions.

G VI: 20 mice; 10 mice: EAC-bearing mice irradiated with blue laser light (high frequency) followed by puls US for 3 minutes and 10 mice: EAC-bearing mice treated with (nano-curcumin) were irradiated with blue laser (high frequency) followed by puls US for 3 minutes.

Nano-curcumin activation

Nano-curcumin activation was achieved through blue laser and/or US irradiation; after mice were anesthetized the probe laser and/or ultrasound was posted nearly the tumor for PDT, SDT, and SPBMT as mentioned before. PDT was applied using a blue diode laser; model LAS-50 Germany and SDT was applied using an ultrasonic instrument; model F-801C China. For assessment treatment; the following analyses were done

Implanted tumor analysis

Tumor growth and/or inhibition were examined regularly every day using a slide digital caliper, then the volume in (mm³) and weight in (g) of the tumor after scarification at the treatment protocol end was calculated.

Biochemical analysis

from all experimental animals, blood samples were withdrawn for obtaining sera for examinations. Malondialdehyde [7,11,13], antioxidant enzymes [7,11], hepatic and renal function tests [7,11] were analyzed in accordance with the manufacturer's kit instructions (BioVision Catalog # K739-100, #K274-100, #K761-100, #K263-100, #K335-100 and #K773-100, Sigma Catalog # MAK179, # MAK080, # MAK052, #MAK055, #MAK089 and #MAK089respectively) using Auto-analyzer; Indiko Plus.

Molecular detection of P21, P16, p53, and TGFβ-1 RT-PCR expression: from the mice, Erich tumor RNA was extracted and full-length cDNA preparation from RNA according to the manufacturer's instruction of QIAGEN kit # K1621, #1622. The followings were added in all PCR tube 5 µl Template P16, P21 and p53 - cDNAs, 10 µl Fermentas# k1081 Green PCR Taq Master Mix (2X) {dNTPs [0.4 mM of each dATP, dCTP, dGTP, dTTP], 0.05u/µl Taq polymerase and reaction buffer}, 1.5 µl of forward and reverse primers: [P21: 5 – *ACGGTGG∇C T TGAC T CGTC* – 3, P21: 5 – *CAGAGTGC∇GACAGCGAC∇G* – 3, P16: 5– T *GGCC∇GAGCGGGGACA* – 3, P16: 5– *GCGGGCTGAGGCGGA T TA* – 3, P53: 5 – *TGCTCACCTGGCT∇AG T* – 3, P53: 5– *∇TGTCTCTGGCTCAGAGG* – 3, TGFβ-1:5– *GTCTGGC T AGCTGTC T* – 3, TGFβ-1: 5 – *A T CATAGGCTGTGACGC* – 3] and final volume 20 µl completed by RNase free deionized water. In all PCR tubes the mixtures were vortexed gently, centrifuged briefly for all drops collection in tubes, then in the Little Genius, Bioer Co thermal cycler, all PCR tubes were placed. The 35 thermal

amplification cycles thermal profile of PCR: 94°C/2min pre-denaturation, followed by 94°C/1min denaturation, 52°C/1min annealing, and 72°C/1min extension, and 72°C/7min last extension. For verification of mRNA preparation + ve control Glyceraldehyde-3-phosphate dehydrogenase (GAPDH):5 – *AGGCGGTGCTGAGTATGTC* – 3, GAPDH: 5– *TGCTGC T CACAC T CT* – 3 was used as, also -ve controls reaction tube without cDNA sample addition and containing no cDNA control template was included. 2% agarose gel was stained with ethidium bromide (EthBr) was used for amplicons analysis and visualized under 302nm BIO-RAD, USA,UV transilluminator for 213 bp, 200 bp, 208 bp, and 530bp bands using Fermentas, 100bp DNA ladder #SM0323.

Histopathological analysis

Excised tumor tissues were properly fixed, and stained by eosin and haematoxylin (H&E) for light microscopy examination.

Transmission Electron Microscope (TEM) ultrastructure analysis

Excised tumor tissues were properly fixed, stained and prepared for semi-thin section examination. Ultra-thin sections prepared using LKB automatic ultra-microtome, mounted on grids, examined by JEOL-100 CX-TEM.

Statistical analysis:

The data were processed using the SPSS program.

Results

Nano-curcumin was successfully synthesized in agreement with other studies according to UV-vis optimum absorption peak, PL optimum photoluminescence peak, XRD crystallinity and purity nature, FTIR bands obtained corresponding to the respective vibrations of the functional groups present in nanocurcumin in addition the shape and size by TEM, **Figure (1.a.)**.

Nano-curcumin without activation has a slight effect on tumor growth and mass inhibition. At 7 days, all modalities have an increasing impact on tumor volume and weight reduction. Upon the second week, the use of blue laser and pulse or continuous US waves with and without nano-curcumin becomes more efficient.

The nano-curcumin presence increases both the blue laser (PDT) and the US (SDT) effectiveness. The obtained results elucidated that puls US is more efficient than cont US in the presence and absence of nano-curcumin. Pulsed ultrasound waves were selected for integration with blue laser at high frequency. The combined therapeutic method is more efficient than using blue laser or ultrasound alone **Figure (1.b. – 1.e.)**.

Oxidative Stress and Antioxidant Status: Increase in MDA; a lipid peroxidation marker was assessed in the EAC-control group. The statistical significant elevation of MDA levels in all radiation-exposed groups and treated without nano-curcumin was observed.

Experimental irradiated study groups with blue laser, US or both in the presence of nano-curcumin showed significantly MDA lower levels compared with both cancer control group, and non-activated nano-curcumin treated group, **Figure (2.a.)**. Also, in the same figure, mice implanted with EAC showed significantly decreased antioxidant activity (CAT, SOD, GST, GR, and TAC) compared with the normal control group. Meanwhile, non-enzymatic and enzymatic antioxidants significantly increase in groups irradiated with either blue laser and/or US both in with and without nano-curcumin compared to the control group of cancer or with mice groups treated without activation nano-curcumin.

Liver and Kidney Function Tests: Kidney function tests, namely: urea and creatinine, are estimated. It was found that kidney function tests increased in all EAC-bearing animal groups. Meanwhile, nano-curcumin caused low levels of creatinine in serum and urea, which may be indicative of renal protection, **Figure (2.b.)**. This also underlines the nano-curcumin renal protective role. Transaminases, alkaline phosphatase, and gamma-glutamyl transferase were also examined. EAC results in significant elevation of serum activity of gamma-glutamyl transferase, transaminases, and alkaline phosphatase in tumor-bearing groups. While, decrease in serum levels of transaminases, gamma-glutamyl transferase and alkaline phosphatase in the EAC treated groups with nano-curcumin, was observed, indicating the activated nano-curcumin hepatic protection, this also underlines the nano-curcumin hepatic protective role.

P21, p16, p53, and TGF β -1 gene expressions: Amplification of p21, p16, p53, and TGF β -1 gene expressions in EAC excised from treated and untreated animals using RT-PCR is illustrated **Figure (3)**. P21, p16, p53, and TGF β -1 PCR amplicons were detected using 2% agarose gel. Products for gene expression of p21, p16, p53, TGF β -1, and GADPH were at 213, 200, 208, 495, and 530bp, respectively. All samples showed positive expression to GADPH. Samples of lanes (1–3, 4–6, 7–9, and 10–12) showed positive bands for p21, p16, p53, and TGF β -1 gene expressions with different intensities with different-studied modalities.

Histological Evaluation: All EAC tumors in the cancerous control group without treatment showed aggressive malignancy with little necrosis. All EAC tumors from groups administered (nano-curcumin only) as sono-photosensitizer; nearly equivalent results as the EAC group owing to nano-curcumin inactivation. All EAC tumors from groups exposed to the blue laser group, low frequency, high frequency only, showed 45–60%, respectively necrotic areas. In the EAC tumors from groups administered (nano-curcumin) and exposed to low frequency, the high frequency showed (65–75%, respectively) necrotic areas. All EAC tumors from groups exposed to puls or cont ultrasound showed (60–65%, respectively) necrotic areas. All EAC tumors from groups were administered (nano-curcumin), and exposed to puls or cont ultrasound showed (75–80%, respectively) necrotic areas. In the case of EAC tumors from

combination groups, high frequency followed by puls ultrasound, with and without (nano-curcumin) administration showed large foci of necrosis areas (85–90%, respectively), **Figure (4.a.)**.

TEM Ultrastructure Evaluation: TEM; the histological evaluation **Figure (4.b.)** revealed that EAC tumors from groups without treatment has shown an irregular serrated nuclear membrane with deep indentations, having large polypoid nuclei, and coarsely clumped dense heterochromatin situated on the nuclear membrane, while in the case of the combination group injected with (nano-curcumin) tumors showed massive areas of dead cell seen as ghosts of pale cells without nuclei and cells having swollen ruptured organelles.

Discussion

In the present manuscript, nano-curcumin was demonstrated as a sensitizer for both blue laser and ultrasound and to determine whether photodynamic therapy and sonodynamic therapy alone or together can be managed safely, providing an increasingly toxic response to carcinogenic cells locally also offer a promising way for cancer eradication. The evaluation of MDA is used as an oxidative stress marker, indicating the role of lipid peroxide in cancer development.

Free radical oxidize polyunsaturated lipids, resulting in MDA, one of the reactive electrophile species, causing cells toxic stress [14,15]. The probable cause of MDA elevated level in cancer could be a deteriorated oxidant-antioxidant balance system that accumulates cancerous tissues with lipid peroxides followed by secretion into the bloodstream [16]. Highly cytotoxic MDA is the major polyunsaturated lipid oxidation aldehyde final peroxy radical product. Reported to inhibit protective enzymes; thus it can have a tumorigenic impact [17]. In this work, MDA elevation in the EAC untreated cancerous control group was reported. MDA levels increase in EAC animal groups when compared to the normal untreated group. Oxidative stress Inhibition by nano-curcumin is mainly due to the trapping of ROS causing peroxidation [18,19].

Animal groups administered nano-chromium as a treatment showed significantly MDA lower level compared with non-nano-treated curcumin groups. These are achieved by the anti-lipid peroxidation characteristic of nano-curcumin through searching for and scavenge free radical generated. Prevention of cellular destruction by ROS results from the anti-oxidant defense system.

The antioxidant defensive system can reveal free radicals, which of great significance value in oxidative stress initiation and MDA formation, thus protecting cancer development [20]. Defense system function through non-enzymatic components (mainly GSH) and enzymatic (including GPx, SOD, CAT, and GST) [21]. SOD is the defense mechanism primary step involving the oxidant-antioxidant system resisting oxidative stress, catalyzes superoxide anion (O_2^-) breaks down into H_2O_2 and O_2 . H_2O_2 can be deleted and converted it into harmless byproducts by Gpx and catalase, thus allowing protection against ROS [22].

GPX is highly effective in free radical neutralization reacting in ROS stress response to peroxides and hydroxoids detoxification that leads to GSH oxidation [23]. Also, GST catalyzes the association of GSH

thiol functional groups with electrolytic xenobiotic, eliminating or converting the xenobiotic-GSH conjugate [24]. In this interaction, glutathione is converted to oxidized GSSG form and reassembled with NADPH consumption by GR [25]. Non-enzymatic antioxidant inside the cell is GSH [32]. GSH is involved in lots of cellular pathways, including intra and extra compound detoxification and cells conserving against the adverse oxidation effects efficiently by scavenging, removing ROS and/or H₂O₂, and suppressing peroxidation [26].

In this work, studied EAC groups evoked low antioxidant activities. Current data is agreement with reported results [27–29]. It was reported that this subsequent reduction antioxidants because of low expression of this defense system during the destruction of the mammary gland. Meanwhile, a significant enzymatic antioxidant and non-enzymatic increase in custody in animals carried EAC subjected to the nano-curcumin, blue laser and/or US.

This increase because of the competence of nano-curcumin to hinder the synthesis of reactive free radicals, promote the activity of the endogenous defense antioxidant system beyond its ROS trapping moiety, and enhance the lowering of EAC oxidative stress [30]. An elevation of antioxidant enzyme activity in nano-curcumin-treated mice indicates its protective effect [31,32].

In this work, antioxidant activities are inversely related to MDA. The elevated level of MDA can be elucidated by an imbalance in the oxidant-antioxidant defense system with the accumulation of lipid peroxides ROS in the tumor, as noted. In addition, it was reported that a decrease in TAC with a higher MDA level in the cancer group compared to the normal untreated group [33–35].

Creatinine and urea, removed from the bloodstream by the kidneys, are metabolic byproducts to prohibit their accumulation. Elevations of all these indices indicate loss of kidney function [36]. This study indicates that EAC implanted in all mice groups caused kidney function loss compared to normal mice, which is inconsistent with other studies [37–39]. Vital indicators of kidney function, urea, and creatinine have been estimated in our work.

In the present work, nano-curcumin improves kidney function tests as an indicator of kidney protection and evokes the nano-curcumin protective role [40]. The liver is the main organ concerned with the biological transformation of xenobiotic substances. Levels of bilirubin and liver transaminases, ALP, and transferase enzymes consider a reliable marker of liver toxicity [41,42].

Increased transaminases due to leakage from liver-destroyed cells (liver injury) [43]. Alkaline phosphatase and transferase enzyme are linked to the cellular membrane. Elevations of ALP and transferase enzyme activities manifest a condition of liver injury [44]. Vital indications of liver function, liver transaminases, ALP, and transferase were taken in our work.

In this work, implanted mice groups, with EAC significantly increased serum transaminases, ALP, and transferase activity. Transaminases, primarily localized in hepatic cell cytoplasm and mitochondria

[45,46]. In this work, nano-curcumin therapy was treated against elevated levels of serum AST, ALT, ALP, and GGT an indicator of liver protection by nan-curcumin.

In the current work, the molecular study of p21, p16, p53, and TGF β -1 gene expressions as markers for cancer treatment and inhibition of angiogenesis; manifested a significant positive agreement between p53, and p16 gene expressions and treatment modalities in the presence of nano-curcumin on the other hand, a negative agreement between cancer development and p53, and P16 expressions in the untreated cancer group. P16, and p53 gene expressions significantly elevated in sono-photo- biomodulation therapy with (nano-curcumin) exposed mice groups than exposed to PDT-modality or SDT-modality only with (nano-curcumin) alone followed by laser-modality or US-modality only without (nano-curcumin) alone and the lowest expression was among the untreated cancer group. Meanwhile, there was a significantly negative agreement between p21, and TGF β -1 expressions and treatment modalities of in the presence of nano-curcumin while a positive agreement between cancer development and p21, and TGF β -1 expressions in the untreated cancer group. P21, and TGF β -1 gene expressions significantly lower in mice groups treated with sono-photo-biomodulation therapy with (nano-curcumin)] than those treated with PDT- modality or SDT-modality only with (nano-curcumin) alone followed by laser-modality or US-modality only without (nano-curcumin) alone and the highest expression was among the untreated cancer group.

The present work indicated that P21, P16, p53, and TGF β -1 gene expressions using RT-PCR a good predictor of cancer treatment and inhibition of angiogenesis and was inconsistent with other studies done by other authors [47– 55]. In the end, the application of photo- and sono- activated phytochemical nanoparticle (nano-curcumin) as in vivo anti-tumor therapy opens up a new way of research in cancer treatment.

Also, the application of nanoparticles enables the great potential for effective drug delivery, allows targeted treatment, improves and amplifies the response to sono-phototherapy.

Recommendation:

Current work offered new trends for the treatment of cancer that require investigations furthermore. More experimental study protocol investigations needed to be introduced to safely conduct this promising modern method for humans and monitor other biophysical and biochemical indices change.

Conclusion

The current work results displayed the sono-photo-biomodulation method, which uses ultrasound and laser exposure in the presence of nano-curcumin to treat cancerous tumor (Ehrlich) implanted in mice as in vivo experimental model a promising trend for treatment of cancer.

Declarations

Ethics approval and consent to participate

Experimental procedures, animal handling and sampling followed the Guide for the Care and Use of Laboratory Animals, 8th edition (National Research Council, 2011) and were approved by Research ethical Committee (Appendix 2; Guide Principles for Biomedical Research Involving Animals, 2011) of the Medical Research Institute, Alexandria University (Alexandria, Egypt). This study is reported in accordance with ARRIVE guidelines (<https://arriveguidelines.org>).

Consent for publication

The authors agree for publication.

Availability of data and material

All data are available.

Competing interests

The authors declare that there are no conflicts of interest and no competing interest.

Funding

The Science, Technology and Innovation Funding Authority (STDF) in cooperation with The Egyptian Knowledge Bank (EKB)

Authors' contributions

All authors contribute in this work SA and SE design the study, write and revise all the manuscript, SA, HM, AE participate in practical work, MA, AS and MK participate in statistical analysis and figure presentation.

Acknowledgements

We would like to thank all the MRI staff members; without them, it could not been done.

References

1. Zhao, CY, Cheng, R, Yang, Z., Tian, ZM. Nanotechnology for Cancer Therapy Based on Chemotherapy. *Molecules*. 2018;23: 826.doi:10.3390/molecules23040826
2. Blanco, E, Hsiao, A, Mann, AP, Landry, MGF, Meric–Bernstam, M. Ferrari. Nanomedicine in cancer therapy: innovative trends and prospects. *Cancer. Sci*. 2011;102:1247–52.
3. Brodin, NP, Guha, C, Tomé, WA. Photodynamic therapy and its role in combined modality anticancer treatment. *Technol. Cancer. Res. Treat*. 2015;14: 355-68.

4. Wan, GY, Liu, Y, Chen, BW, Liu, YY, Wang, YS, Zhang, N. Recent advances of sonodynamic therapy in cancer treatment. *Cancer. Biol. Med.* 2016;13: 325-38.
5. Dardeer AGE, Hussein NG & Abd El-Kaream SA, New Impacts of *Garcinia Cambogia* as Sono/photosensitizer on Ehrlich Ascites Carcinoma Bearing Mice. *Int J Inf Res Rev*, 2021;8: 7182.
6. Miyoshi, N, Kundu, SK, Tuziuti, T, Yasui, K, Shimada, I, Ito, Y. Combination of Sonodynamic and Photodynamic Therapy against Cancer Would Be Effective through Using a Regulated Size of Nanoparticles. *Nanosci. Nanoeng.* 2016;4: 1–11.
7. Abu Rakhey MMM, Abd El-Kaream SA, Daoxin Ma. Folic Acid Conjugated Graphene Oxide Graviola Nanoparticle for Sono-Photodynamic Leukemia Treatment: Up-To-Date Cancer Treatment Modality. *J Biosci Appl Res*, 2022;8: 28-45.
8. Aditya, NP, Hamilton, IE, Norton, IT. Amorphous nano-curcumin stabilized oil in water emulsion: Physicochemical characterization. *Food Chem.* 2017;224: 191–200.
9. Devara, RK, Mohammad, HUR, Rambabu, B, Aukunuru, J, Habibuddin, M. Preparation, optimization and evaluation of intravenous curcumin nanosuspension intended to treat liver fibrosis. *Turkish J. Pharma. Sci.* 2015;12: 207-20.
10. [10] Yallapu MM, Jaggi, M, Chauhan, SC. Curcumin Nanomedicine: A Road to Cancer Therapeutics. *Curr. Pharm. Des.* 2013;19: 1994–2010.
11. Abd El-Kaream, SA. Biochemical and biophysical study of chemopreventive and chemotherapeutic anti-tumor potential of some Egyptian plant extracts. *Biochem. Biophys. Rep.* 2019;18: 100637.
12. [12] Gopal, J, Muthu, M, Chun, SC. Water soluble nanocurcumin extracted from turmeric challenging microflora from human oral cavity. *Food Chem.* 2016,211: 903-9.
13. Khedr Y, Kotb M, Abd El-Kaream SA & El-Bayady O, Assessment of Some Biochemical Parameters and Dielectric Relaxations in β -Thalassemic Children. *Curr Appl Sci Technol*, 2020;20: 408.
14. Rao, CSS, Kumari, DS. Changes in plasma lipid peroxidation and the antioxidant system in women with breast cancer. *Int. J. Basic. Appl. Sci.* 2012;1: 429-38.
15. Dardeer AGE, Hussein NG & Abd El-Kaream SA, New *Garcinia Cambogia* as Sono/Photosensitizer on Ehrlich Ascites Carcinoma Bearing Mice in Presence of Dieldrin Pesticide as an Environmental Pollutant. *Int J Innov Sci Res*, 2021;10: 1583.
16. Ziech, D, Franco, R, Georgakilas, AG, Georgakila, S, Malamou-Mitsi, V, Schoneveld, O. The role of reactive oxygen species and oxidative stress in environmental carcinogenesis and biomarker development. *Chem. Biol. Interact.* 2010;188: 334-9.
17. Naser, B, Bodinet, C, Tegtmeier, M, Lindequist, U. *Thuja occidentalis* (*Arbor vitae*): A Review of its Pharmaceutical, Pharmacological and Clinical Properties. *eCAM.* 2005;2: 69–78.
18. López-Lázaro, M. Anticancer and carcinogenic properties of curcumin: Considerations for its clinical development as a cancer chemo preventive and chemotherapeutic agent. *Mol. Nut. Food. Res.* 2008;52: 103-27.

19. Abd El-Kaream, SA, Abd Elsamie, GH, Abd-Alkareem AS. Sono-photodynamic modality for cancer treatment using bio-degradable bio-conjugated sonnelux nanocomposite in tumor-bearing mice: Activated cancer therapy using light and ultrasound. *Biochem. Biophys. Res. Commun.* 2018;503: 1075-1086.
20. Abdulrahman JM, Hosny Hosny G & Abd El-Kaream SA, The effectiveness of nano-chlorophyll in breast cancer-targeted therapy. *J Biosci Appl Res*, 2018;4: 331.
21. Vázquez-Garzón, V, Arellanes-Robledo, J, García-Román, R, Aparicio-Rautista, DI, Villa-Treviño, S. Inhibition of reactive oxygen species and pre-neoplastic lesions by quercetin through an antioxidant defense mechanism. *Free. Radic. Res.* 2009;43: 128-37.
22. Usunomena, U, Ademuyiwa, A, Tinuade, O, Uduenevwo, F, Martin, O, Okolie, N. N-nitrosodimethylamine (NDMA), liver function enzymes, renal function parameters and oxidative stress parameters: A Review. *Br. J. Pharmacol. Toxicol.* 2012;3: 165-76.
23. Rao, G, Rao, C, Pushpangadan, P, Shirwaikar, A. Hepatoprotective effects of rubiadin, a major constituent of *Rubiocordifolia* Linn. *J. Ethnopharmacol.* 2006;103: 484-90.
24. Revathi, R, Manju, V. The effects of Umbelliferone on lipid peroxidation and antioxidant status in diethylnitrosamine induced hepatocellular carcinoma. *J. Acute. Medicine.* 2013;3:73-82.
25. Wu, G, Fang, YZ, Yang, S, Lupton, JR, Turner, ND. Glutathione metabolism and its implications for health. *J. Nutr.* 2004;134: 489-92.
26. Blair, IA. Endogenous glutathione adducts. *Curr. Drug. Metab.* 2006;7: 853-72.
27. Ghosh, D, Choudhury, ST, Ghosh, S, Mandal, AK, Sarkar, S, Ghosh, A. Nano capsulated curcumin: Oral chemopreventive formulation against diethylnitrosamine induced hepatocellular carcinoma in rat. *Chem. Biol. Interact.* 2012;195: 206-14.
28. Pradeep, K, Mohen, CV, Gobian, K, Karthikeyan, S. Silymarin modulates the oxidant-antioxidant imbalance during diethylnitrosamine induced oxidative stress in rats. *Eur. J. Pharmacol.* 2007;560: 110-16.
29. Rajeshkumar, N, Kuttan, R. Inhibition of N-nitrosodiethylamine induced hepatocarcinogenesis by Picroliv. *J. Exp. Clin. Cancer. Res.* 2000;19: 459-65.
30. Abd El-Kaream SA, Abd Elsamie, GH, Isewid, GA. Laser and Ultrasound Activated Photolon Nanocomposite in Tumor-Bearing Mice: New Cancer Fighting Drug-Technique. *Arch. Oncol. Cancer Ther.* 2019;2: 1-15.
31. Ren, W, Qiao, Z, Wang, H, Zhu, L, Zhang, L. Flavonoids: promising anticancer agents. *Med. Res. Rev.* 2003;23: 519-34.
32. Bishayee, K, Ghosh, S, Mukherjee, A, Sadhukhan, R, Mondal, JK, Bukhsh, AR. Quercetin induces cytochrome-c release and ROS accumulation to promote apoptosis and arrest the cell cycle in G2/ M, in cervical carcinoma: signal cascade and drug-DNA interaction. *Cell. Prolif.* 2013;46:153-63.
33. Kuno, T, Tsukamoto, T, Hara, A, Tanaka, T. Cancer chemoprevention through the induction of apoptosis by natural compounds. *J. Biophys. Chem.* 2012;3:156-73.

34. Kumaraguruparan, R, Subapriya, R, Kabalimoorthy, J, Nagini, S. Antioxidant profile in the circulation of patients with fibroadenoma and adenocarcinoma of the breast. *Clin. Biochem.* 2002;35: 275-9.
35. Sener, D, Gönenç, A, Akinci, M, Torun, M. Lipid peroxidation and total antioxidant status in patients with breast cancer. *Cell. Biochem. Funct.* 2007;25: 377-82.
36. Abd El-Kaream, SA, Abd Elsamie, GH, Abbas, AJ. Sono and photo sensitized gallium-porphyrin nanocomposite in tumor-bearing mice: new concept of cancer treatment. *Am. J. Nanotechnol. Nanomed.* 2019;2: 5-13.
37. Han, W, Bonventre, J. Biologic markers for the early detection of acute kidney injury. *Curr. Opin. Crit. Care.* 2004;10: 476–82.
38. Sharma, V, Paliwal, R, Janmeda, P, Sharma, SH. The reno-protective efficacy of *Moringa oleifera* pods on xenobiotic enzymes and antioxidant status against 7,12-dimethylbenz[a]anthracene exposed mice. *J. Chin. Integr. Med.* 2012;10: 1171-8.
39. Paliwal, R, Sharma, V, Pracheta, S, Sharma, Yadav, S, Sharma, SH. Antinephrotoxic effect of administration of *Moringa oleifera* Lam. in amelioration of DMBA-induced renal carcinogenesis in Swiss albino mice. *Biol. Med.* 2011;3: 27-35.
40. Abd El-Kaream, SA, Abd Elsamie, GH, Metwally, MA, Al-mamoori, AYK. Sono and photo stimulated chlorine e6 nanocomposite in tumor-bearing mice: upcoming cancer treatment. *Radiol. Med. Diag. Imag.* 2019;2: 1-11.
41. George, G, Wakasi, M, Egoro, E. Creatinine and urea levels as critical markers in end-stage renal failure Research and Review. *J. Med. Heal. Sci.* 2014;3: 41-4.
42. Singh, A, Bhat, TK, Sharma, OM. Clinical biochemistry of hepatotoxicity. *J. Clinic. Toxicol.* 2011;4: 1-19.
43. [43] Boone, L, Meyer, D, Cusick, P, Ennulat, D, Bolliger, AP, Everds, N. Selection and interpretation of clinical pathology indicators of hepatic injury in preclinical studies. *Vet. Clin. Pathol.* 2005;34: 182-8.
44. Ozer, J, Ratner, M, Shaw, M, Bailey, W, Schomaker, S. The current state of serum biomarkers of hepatotoxicity. *Toxicology.* 2008;245: 194-205.
45. Ramaiah, S. A toxicologist guide to the diagnostic interpretation of hepatic biochemical parameters. *Food. Chem. Toxicol.* 2007;45: 1551–7.
46. Amacher, D. A toxicologist's guide to biomarkers of hepatic response. *Hum. Exp. Toxicol.* 2002;21: 253-62.
47. El Dine RSS & Abd El-kaream SA. Therapeutic effects of laser on the stiffness of the Achilles tendon mammalian muscles. *Romanian J. Biophys* 2015;25:. 47-62
48. Sharpless, NE, Alson, S, Chan, S, Silver, DP, Castrillon, DH, DePinho, RA. p16 INK4a and p53 deficiency cooperate in tumorigenesis. *Cancer Res.* 2002;62: 2761-5.
49. El Dine RSS, Abd El-kaream SA, Elkholy SM, Abd El maniem, NA. Comparative study for the therapeutic effect of shark care and 5-fluorouracil drugs in mice with hepatocellular carcinoma in the presence of electric field. *Am. J. Biomed. Sci.* 2015;7: 76-97.

50. Mostafa M, Oday S, Henaish AM, Abd El-Kaream SA, Ghazy R, Hemeda, OM, Dorgham AM, Al-Ghamdi H; Almuqrin AH, Sayyed MI, Trukhanov SV, Trukhanova EL, Trukhanov AV; Zhou D, Darwish M. AStructure, Morphology and Electrical/Magnetic Properties of Ni-Mg Nano-Ferrites from a New Perspective. *Nanomaterials* 2022;12:1045.
51. Gartel, AL, Radhakrishnan, SK. Lost in transcription: p21 expression mechanisms, and consequences. *Cancer Res.* 2005;65: 3980-5.
52. El Dine RSS & Abd El-kaream SA, Study of the effect of silver nanoparticles encapsulated by doxorubicin drug in the treatment of hepatocellular carcinoma. *J Biosci Appl Res*, 2015;1: 243.
53. Mostafa M, Oday S, El-Shahawy M, Ghazy R, Hemeda, O, Abd El-Kaream S, Dorgham A. Effect of Methyl Cellulose "MC" on some physical properties of Nickel Magnesium Ferrite - MC nanocomposite. *Arab J Nucl Sci Appl.* 2022;55:1-13.
54. Jasim AA, Abdulrahman JM, Abd El-kaream SA, Hosny G. Biochemical and pathological evaluation of the effectiveness of nano-targeted sono-photodynamic therapy in breast cancer. *J. Biosci. Appl. Res.* 2019; 5:18-31.
55. Abdulrahman JM, AbdElsamie GH, Al-rawi RA, Abd El-kaream SA. Anti-tumor synergistic activity of nano-chlorophyll with sonophotodynamic on Ehrlich ascites carcinoma in mice. *Zanco J. Med. Sci.* 2020; 4:132-42.

Figures

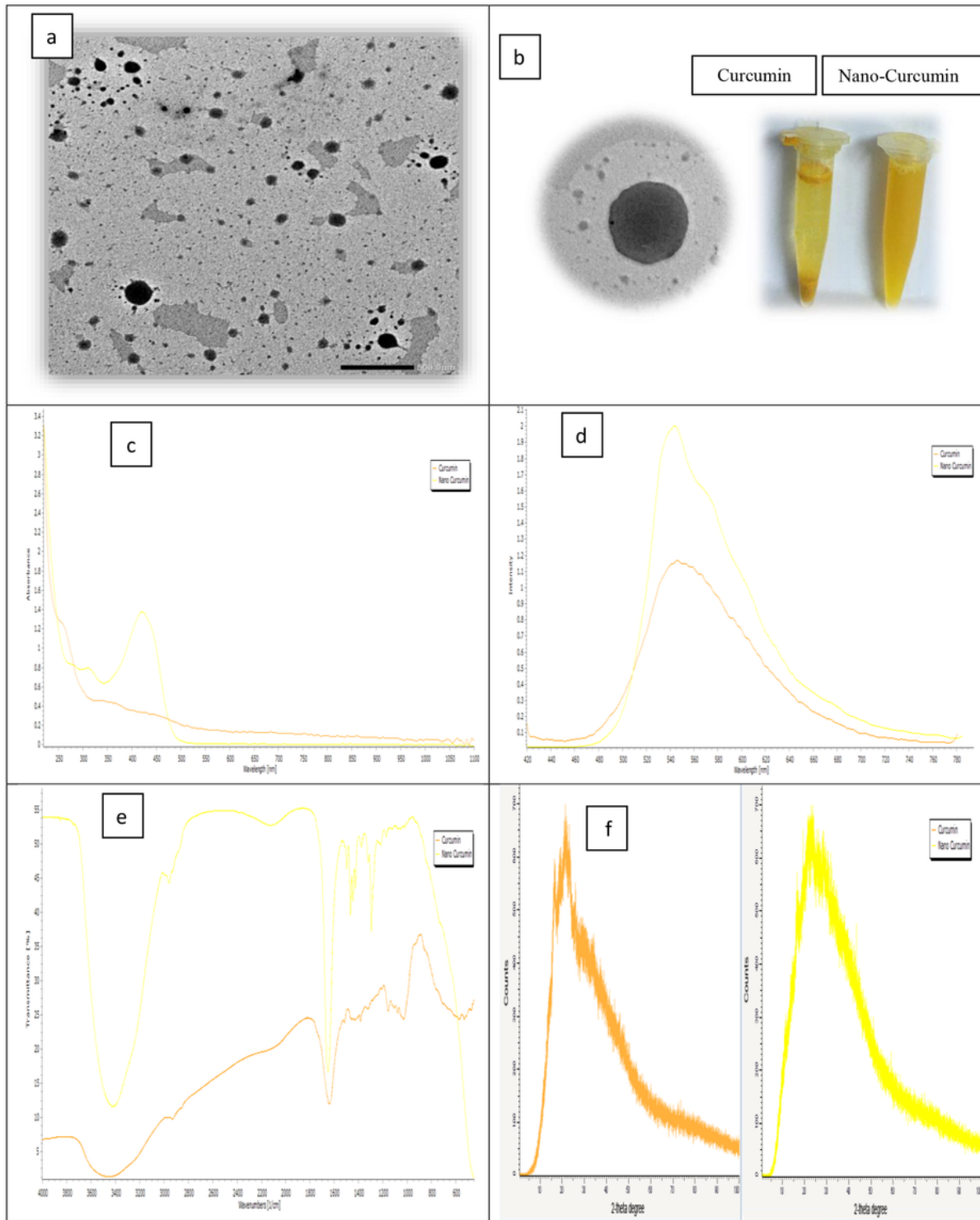


Figure 1

(1.a.): Characterization of synthesized nano-curcumin; (a) TEM, (b) non soluble curcumin vs soluble nano-curcumin, (c) UV-vis spectra, (d) PL spectra, (e) Fourier transform infrared (FTIR) spectra, (f) X-ray powder diffraction (XRPD) pattern.

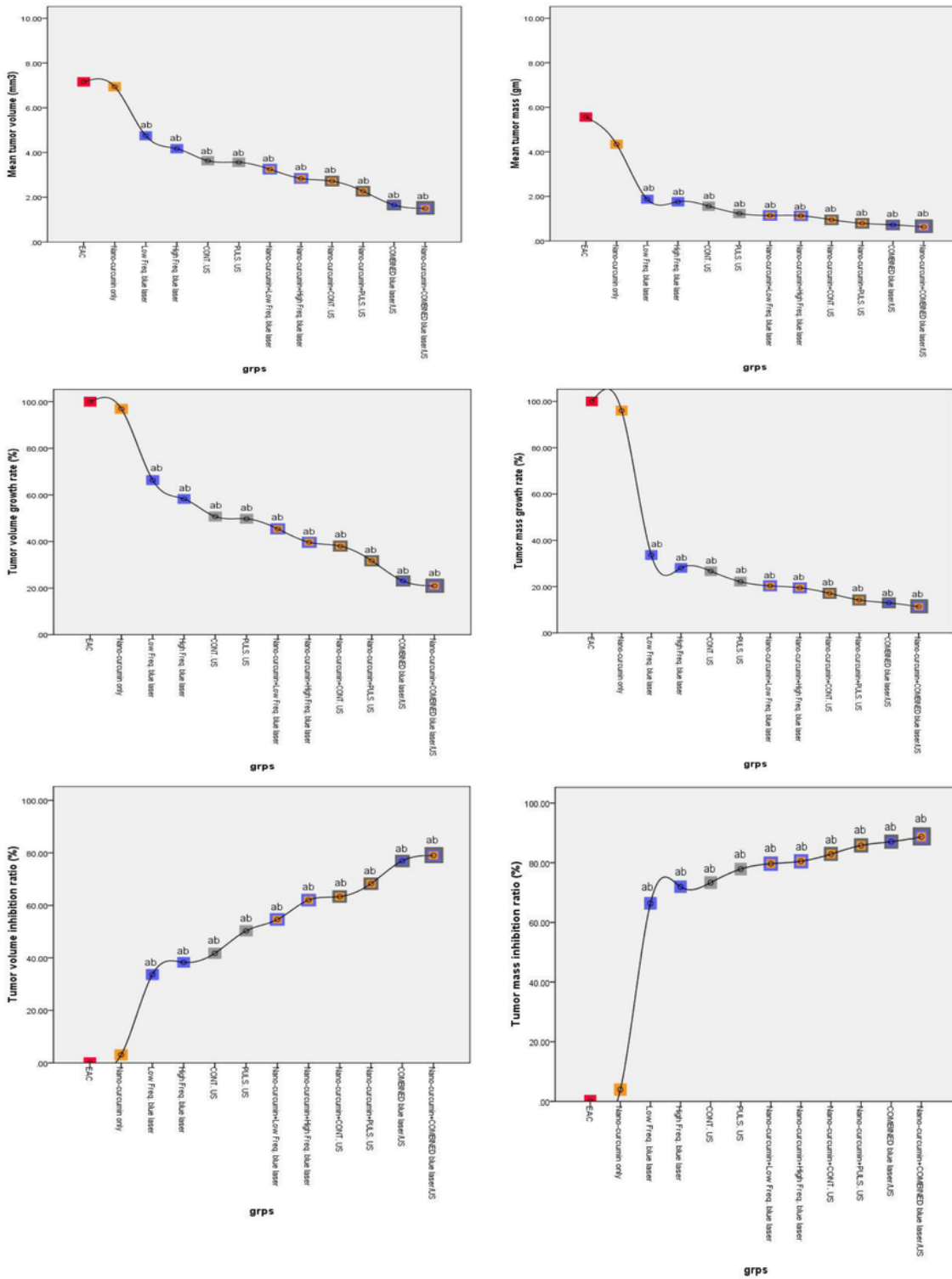


Figure 2

(1.b.): The effect of **blue Laser** at different frequencies, US continuous / pulsed and combined modalities on the tumor volume (mm³), tumor volume growth rate (%), tumor volume inhibition ratio (%), tumor mass (gm), tumor mass growth rate (%), tumor mass inhibition ratio (%), of untreated and nano-curcumin treated groups.

F: F value for ANOVA test (TV (mm³): 27.424 p<0.001*, TM (gm): 20.364 p<0.001*)

a: Significant with EAC group b: Significant with nano-curcumin only group *: Statistically significant at p ≤ 0.05

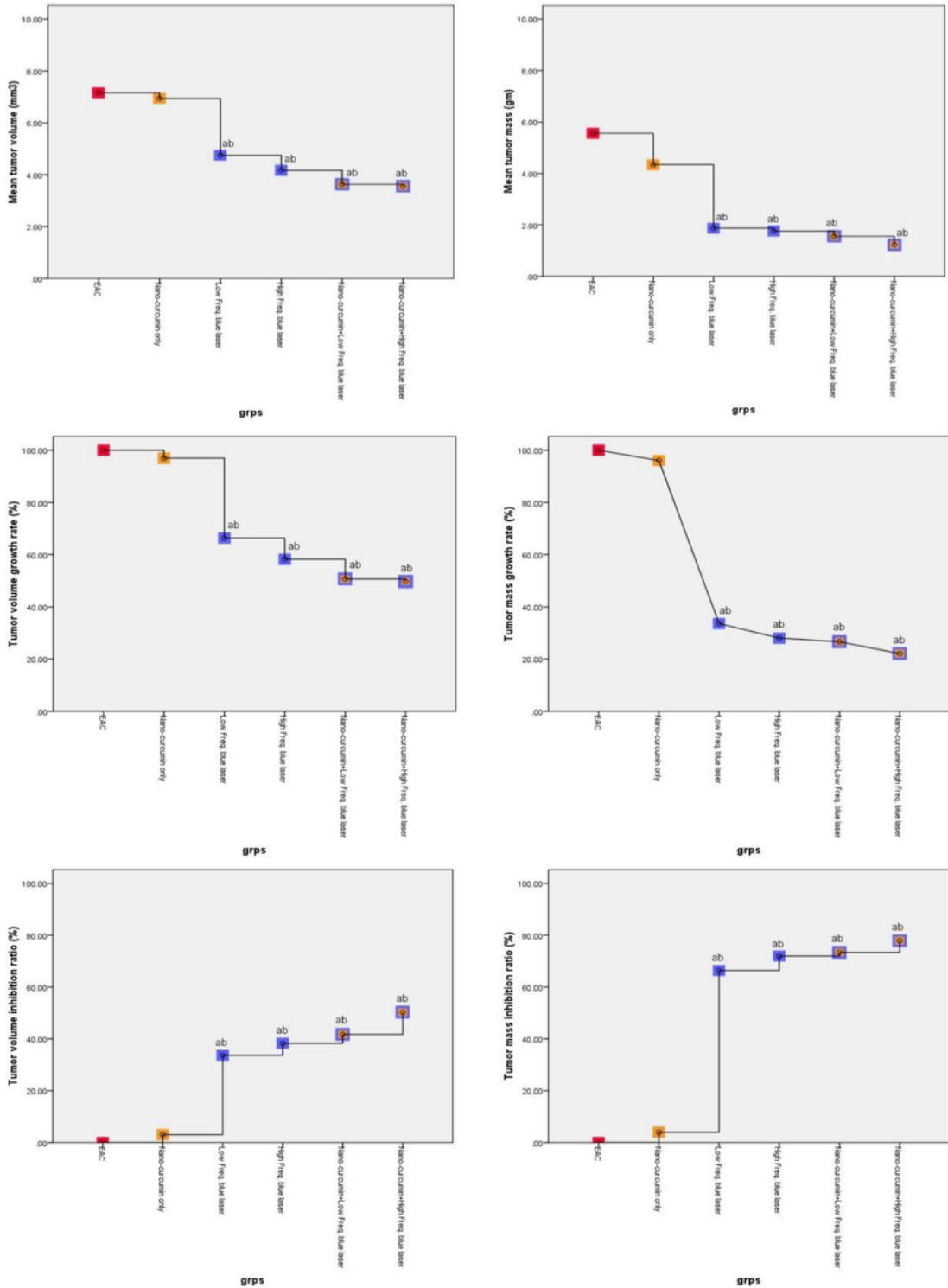


Figure 3

(1.c.): The effect of **blue Laser at different frequencies** on the tumor volume (mm³), tumor volume growth rate (%), tumor volume inhibition ratio (%), tumor mass (gm), tumor mass growth rate (%), tumor mass inhibition ratio (%), of untreated and nano-curcumin treated groups.

F: F value for ANOVA test (TV (mm³): 27.424 p<0.001*, TM (gm): 20.364 p<0.001*)

a: Significant with EAC group b: Significant with nano-curcumin only group *: Statistically significant at $p \leq 0.05$

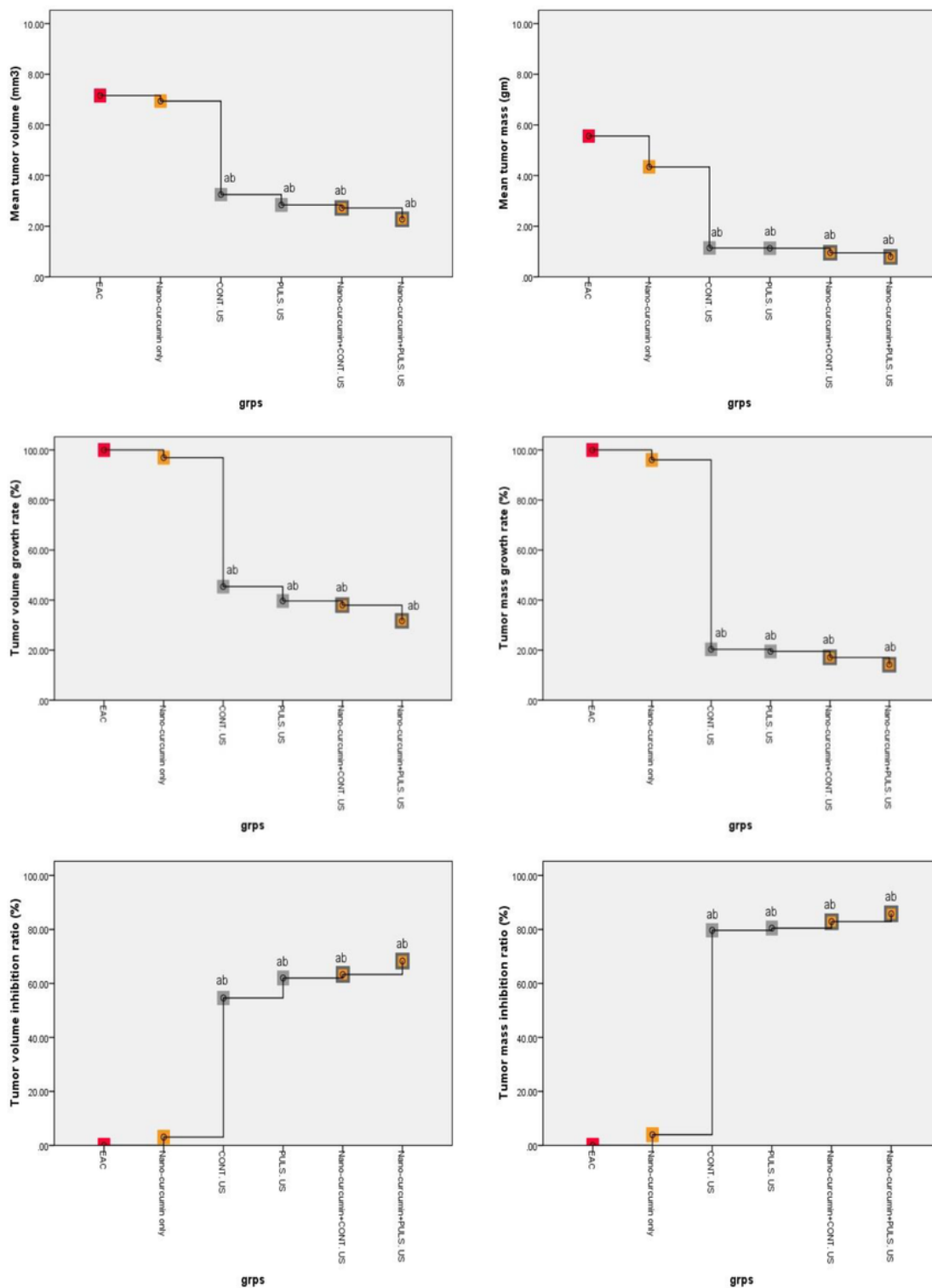


Figure 4

(1.d.): The effect of **continuous / pulsed US** on the tumor volume (mm³), tumor volume growth rate (%), tumor volume inhibition ratio (%), tumor mass (gm), tumor mass growth rate (%), tumor mass inhibition ratio (%), of untreated and nano-curcumin treated groups.

F: F value for ANOVA test (TV (mm³): 27.424 p<0.001*, TM (gm): 20.364 p<0.001*)

a: Significant with EAC group b: Significant with nano-curcumin only group *: Statistically significant at $p \leq 0.05$

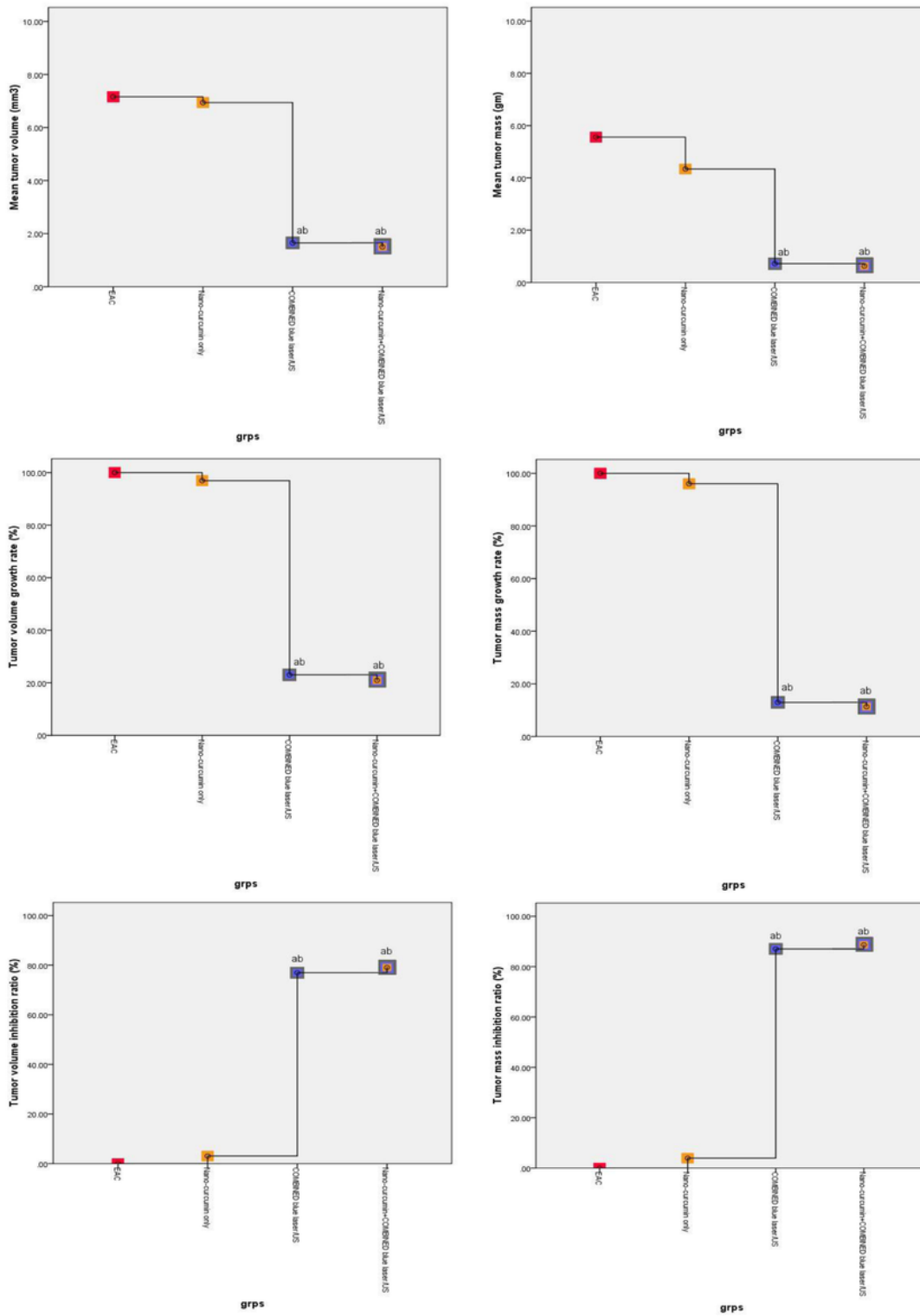


Figure 5

(1.e.): The effect of **blue Laser/US combined** modalities on the tumor volume (mm³), tumor volume growth rate (%), tumor volume inhibition ratio (%), tumor mass (gm), tumor mass growth rate (%), tumor mass inhibition ratio (%), of untreated and nano-curcumin treated groups.

F: F value for ANOVA test (TV (mm³): 27.424 p<0.001*, TM (gm): 20.364 p<0.001*)

a: Significant with EAC group b: Significant with nano-curcumin only group *: Statistically significant at $p \leq 0.05$

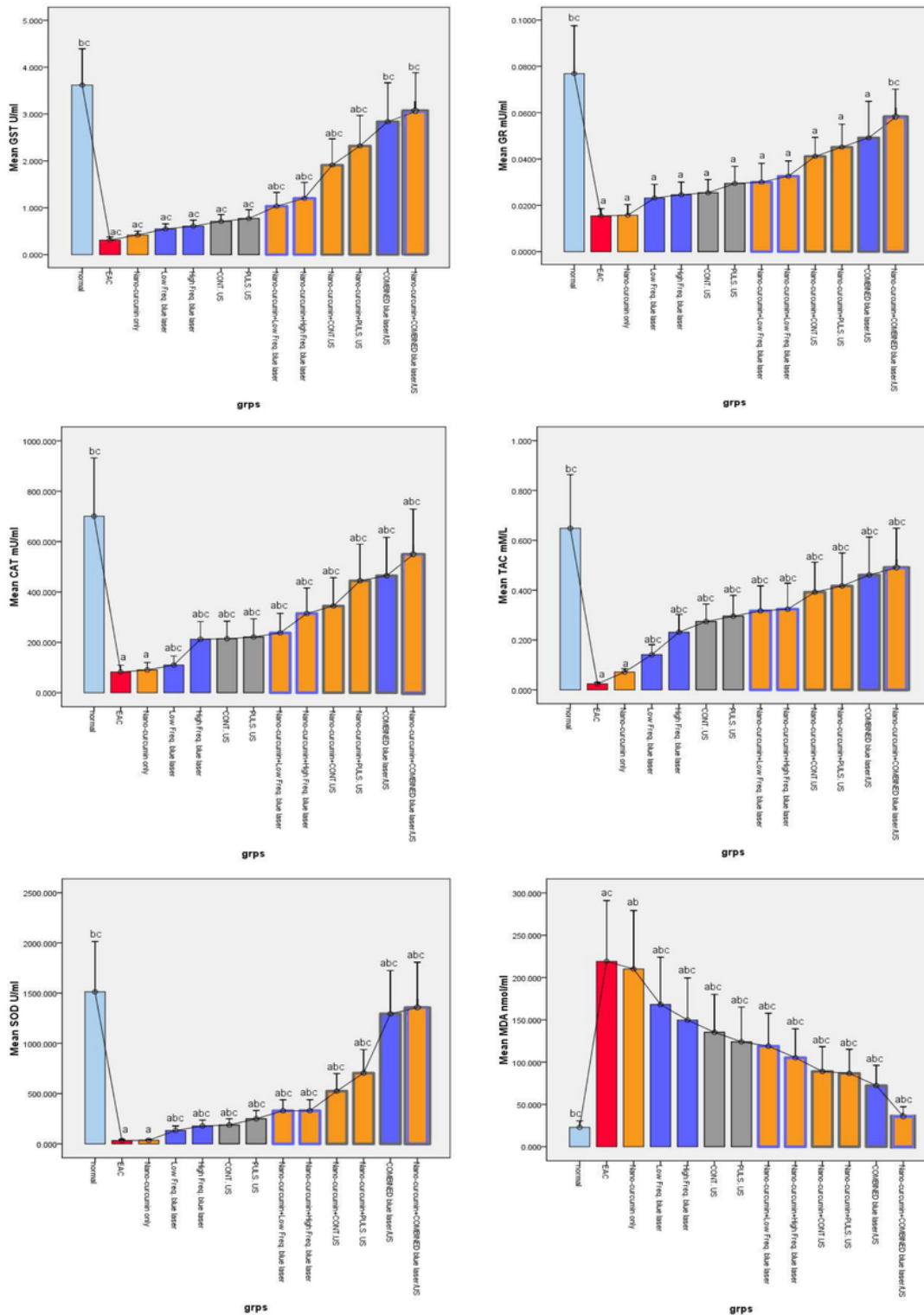


Figure 6

(2.a.): The effect of blue Laser at different frequencies, US continuous / pulsed and combined modalities on antioxidants activities, capacities and MDA, of untreated and nano-curcumin treated groups. F: value for ANOVA test (GST (U/ml): 65.121 $p < 0.001^*$, GR (mU/ml): 7.123 $p < 0.001^*$, CAT (mU/ml): 1486 $p < 0.001^*$, TAC (mM/L): 504.348 $p < 0.001^*$, SOD (U/ml): 30050 $p < 0.001^*$ and MDA (nmol/ml): 1950 $p < 0.001^*$)

Data was expressed by using mean \pm SD; a: Significant with Normal group, b: Significant with EAC group, c: Significant with nano-curcumin group, *: Statistically significant at $p \leq 0.05$.

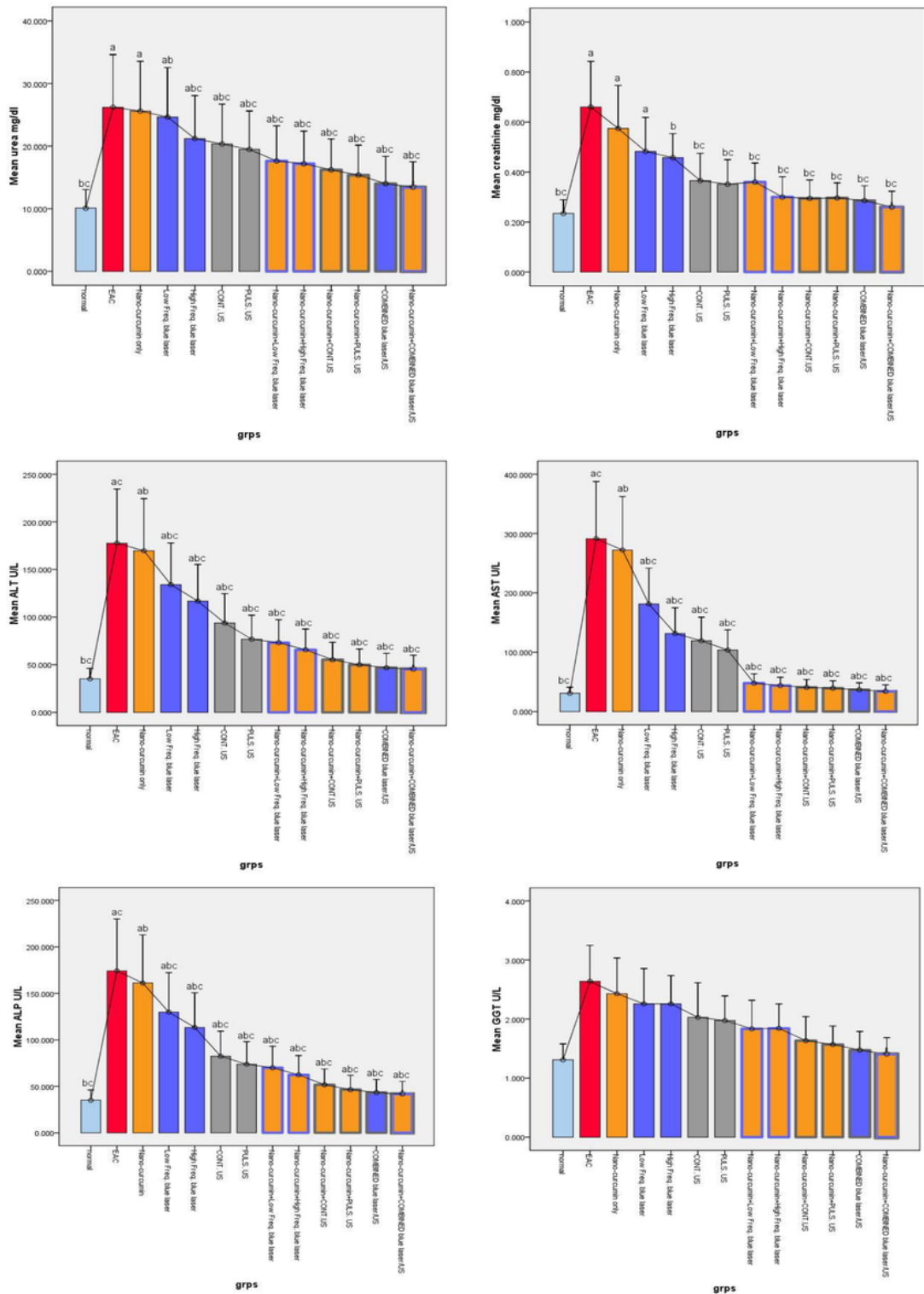


Figure 7

(2.b.): The effect of blue Laser at different frequencies, US continuous / pulsed and combined modalities on renal and hepatic biomarkers, of untreated and nano-curcumin treated groups. F: value for ANOVA test (Urea (mg/dl): 275.140 p<0.001*, Creatinine (mg/dl): 10.560 p<0.001*, ALT (U/l): 457.10 p<0.001*, AST (U/l): 8793 p<0.001*, ALP (U/l): 8683 p<0.001* and GGT (U/l): 4.850 p<0.001*)

Data was expressed by using mean \pm SD; .a: Significant with Normal group, b: Significant with EAC group, c: Significant with nano-curcumin group, *: Statistically significant at $p \leq 0.05$.

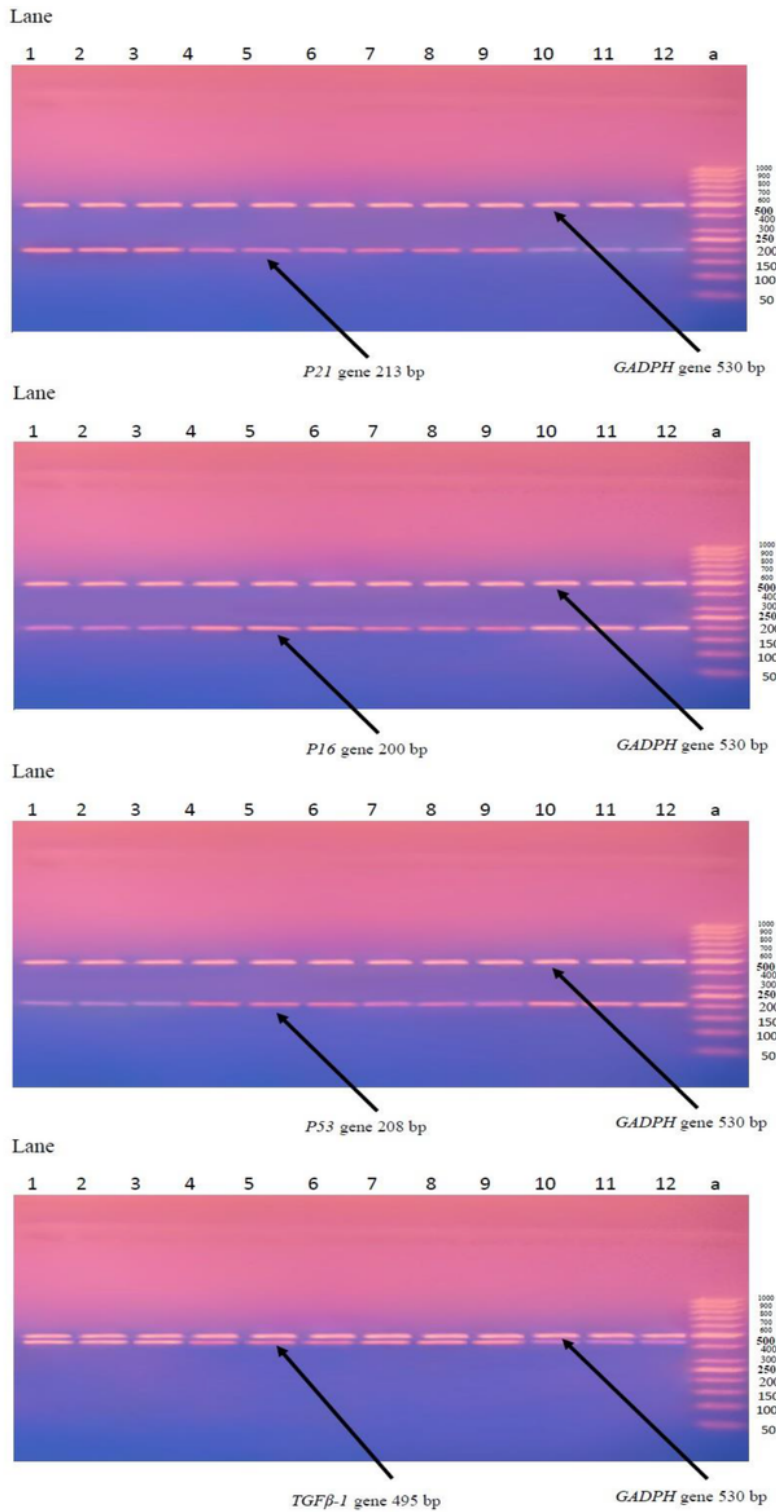


Figure 8

(3): The effect of high freq. blue laser, pulsed US and combined modalities on *p21*, *p16*, *p53* and *TGFβ-1* gene expression levels, of nano-curcumin treated and untreated groups.

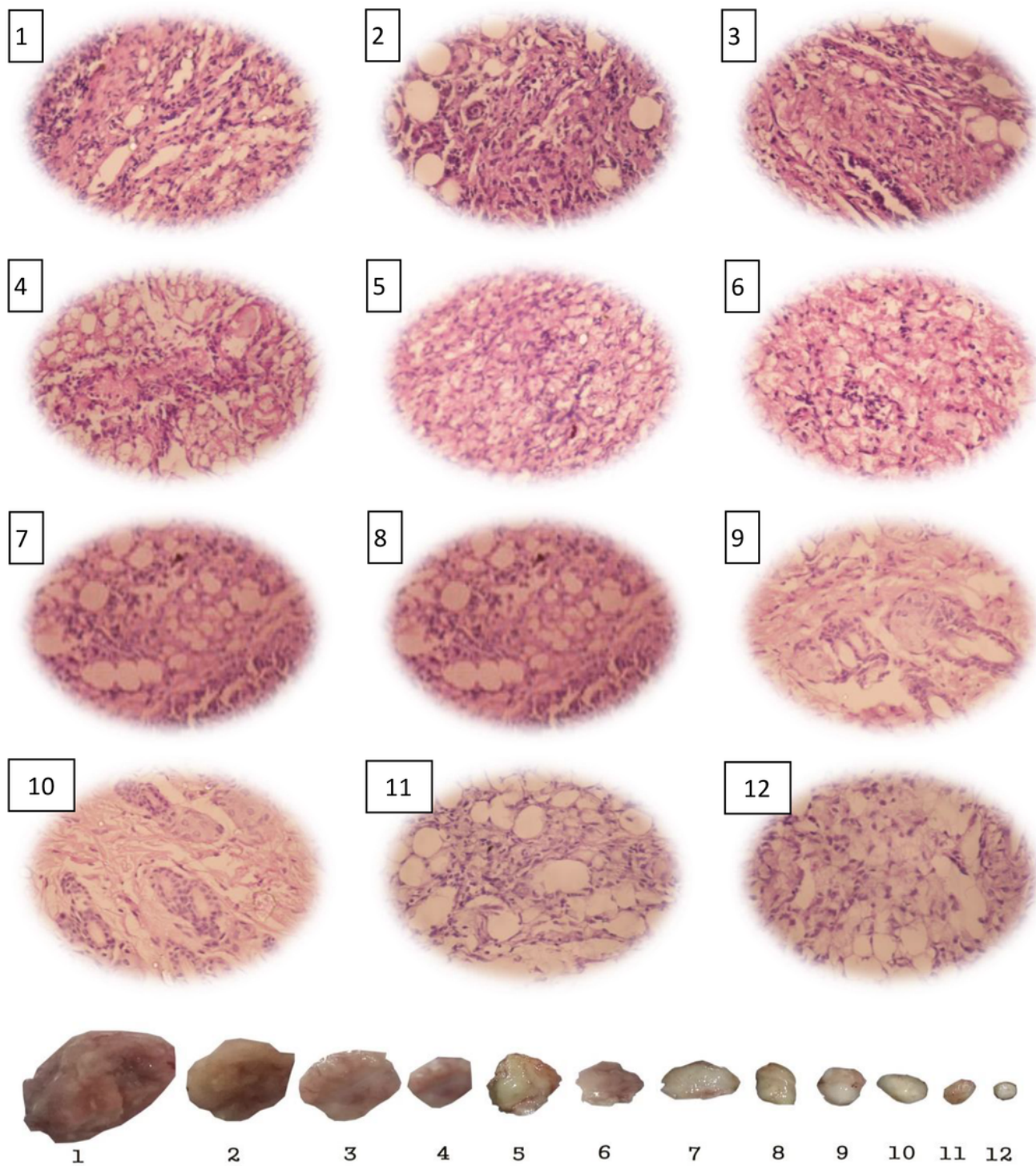


Figure 9

(4.a): Histopathological H&E microscopic examination: (1) untreated EAC implanted without any treatment group, (2) nano-curcumin treated without activation group, (3) low freq. blue Laser irradiated group in absence of nano-curcumin, (4) high freq. blue Laser irradiated group in absence of nano-curcumin, (5) low freq. blue Laser irradiated group in presence of nano-curcumin, (6) high freq. blue Laser irradiated group in presence of nano-curcumin, (7) continuous US irradiated group in absence of nano-

curcumin, (8) pulsed US irradiated group in absence of nano-curcumin, (9) continuous US irradiated group in presence of nano-curcumin, (10) pulsed US irradiated group in presence of nano-curcumin, (11) combined high freq. blue Laser /puls.US irradiated group in absence of nano-curcumin and (12) combined high freq. blue Laser /puls.US irradiated group in presence of nano-curcumin.

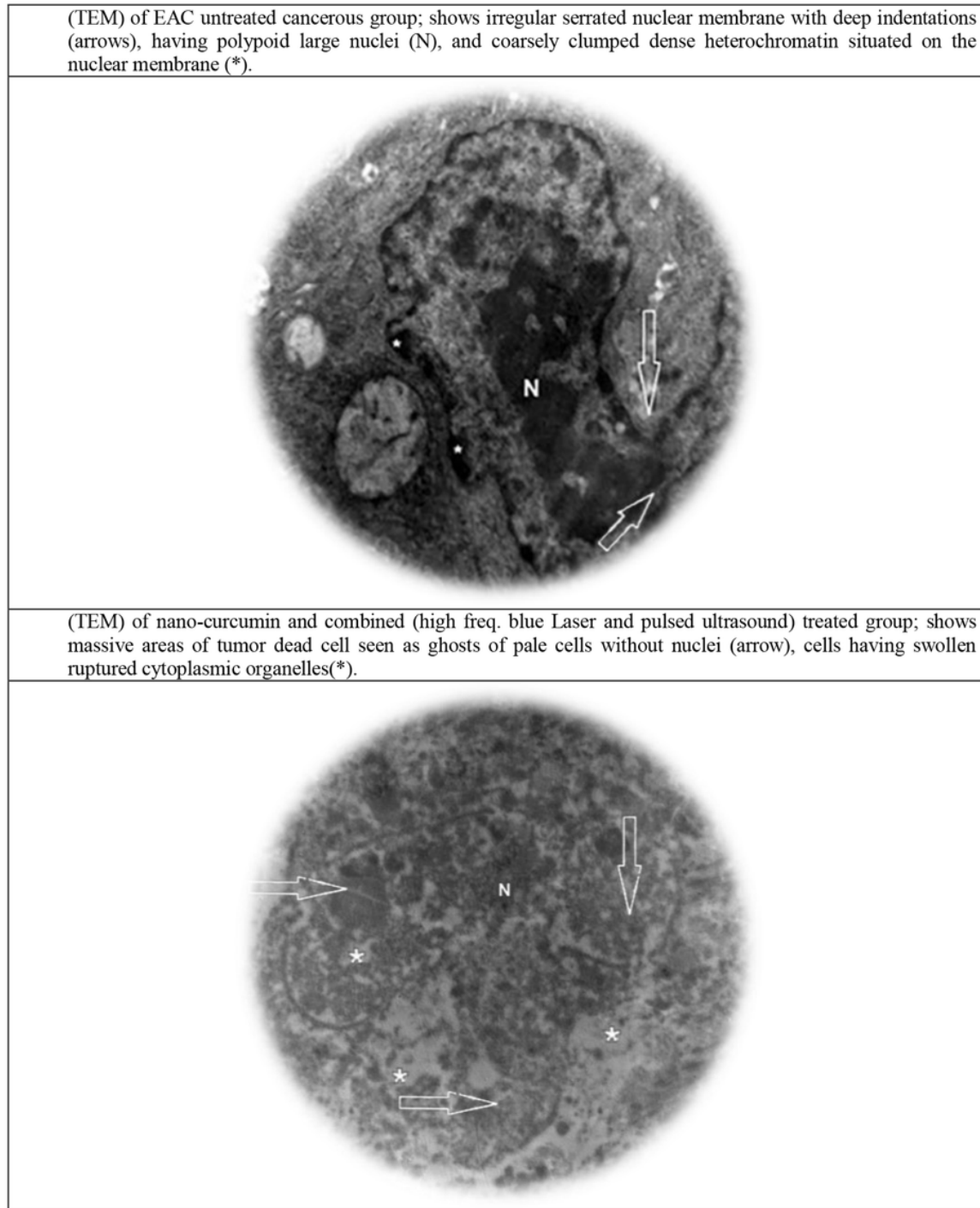


Figure 10

(4.b.): TEM histological ultra-structure evaluation of activated nano-curcumin untreated and treated groups.

Supplementary Files

This is a list of supplementary files associated with this preprint. Click to download.

- [nanocurcumingraphicalabstract.docx](#)